Diurnal rhythmicity in salivary effector expression and metabolism shapes aphid performance on wheat plants

Jinlong Han[1], Daniel Kunk[1,2], Meihua Cui[1], Yoshiahu Goldstein[3], Vered Tzin[3] and Vamsi J. Nalam[1,2*]

[1]Department of Agricultural Biology, Colorado State University, Fort Collins, CO, USA

[2]Department of Cell and Molecular Biology, Colorado State University, Fort Collins, CO, USA

[3]French Associates Institute for Agriculture and Biotechnology of Drylands, Jacob Blaustein Institutes for Desert Research, Ben-Gurion University of the Negev, Midreshet Ben Gurion, Israel

***Corresponding Author:** Vamsi.Nalam@colostate.edu

Keywords:

Diurnal rhythms, aphids, feeding behaviors, salivary effectors, osmoregulation.

Abstract

Diurnal rhythms influence insect behavior and physiology, driving adaptive responses and synchronizing internal processes with daily light-dark cycles. Aphids are important agricultural pests that feed from phloem sieve elements for prolonged periods by delivering a diverse array of salivary effectors to modulate plant responses. Here, we show that the bird cherry-oat aphid (*Rhopalosiphum padi*), an important pest of cereals worldwide, expresses different putative salivary effectors at different times of the day, which may, in part, aid with wheat (*Triticum aestivum*) host colonization. We recorded aphid feeding with the electrical penetration graph (EPG) technique, which revealed diurnal patterns in aphid feeding, particularly extended phloem salivation occurring during early nighttime. Although no diurnal rhythms were detected for phloem sap ingestion, higher honeydew excretion was observed at night. Temporal aphid transcriptome profiles revealed 4,460 diurnally rhythmic transcripts, categorized into four distinct expression clusters linked to various metabolic pathways. Significantly, we identified distinct combinations of putative salivary effectors expressed at different times. Notably, 43% peaked in expression during early nighttime, aligning with the heightened nighttime salivation observed in the aphids using the EPG technique. Silencing key effector genes, which peak in expression at night, impaired aphid feeding and performance on wheat plants without impacting aphid performance on diets. Our study highlights aphid feeding behavior and performance as tightly linked to and influenced by the diurnal expression of salivary effectors and provides the first insights into diurnal feeding behaviors in aphids, revealing opportunities for targeted pest control strategies based on disrupting these rhythms.

Significance Statement

Aphids are among the most destructive pests on crops, threatening food security worldwide. While diurnal rhythms in crops and their aphid pests have been briefly explored, our understanding of how these rhythms ultimately shape the plant-aphid relationship is unknown. Here, we report for the first time that aphids exhibit diurnal rhythms in feeding behaviors, salivary effector expression, and metabolism. A broadened understanding of the presence and role of diurnal rhythms in aphids offers new insights into how behavioral and molecular factors influence the plant-aphid relationship. This temporal insight into aphid biology has the potential to aid in the development of targeted pest management strategies that disrupt an aphid's interaction with its host, thereby minimizing crop damage and yield loss.

Introduction

The recurring cycles of day and night caused by Earth's daily rotation profoundly influence all life, including plants and their pests. All living organisms have evolved internal biological clocks (i.e., circadian clocks) to anticipate and respond to cyclical changes in their environments by orchestrating various physiological and behavioral processes (1). Diurnal and circadian rhythms entail daily biological cycles, with circadian rhythms representing a subset characterized by internally sustained oscillations persisting even without external cues (2). Our understanding of these rhythms has led to profound insights into mechanisms governing the intricate biological processes that shape various daily and seasonal behavioral patterns in diverse taxa, including insects and plants. Despite a significant body of knowledge on diurnal rhythms in model organisms and host-parasite interactions (3, 4), research on agricultural pests and their interactions with plant hosts remains largely underexplored. Given the significant threat pests pose to crop production, deciphering the temporal aspects of their behavior, physiology, and gene expression is a crucial step toward developing more effective pest control strategies (5, 6).

Aphids are among the most devastating pests worldwide, causing significant damage to various economically important crops through their consumption of sugar-rich phloem sap, delivery of phytotoxic salivary secretions, transmission of plant-pathogenic viruses, and promoting the growth of sooty-mold on their sugar-rich excrement (7). Studies on circadian clock-regulated plant defenses against arthropod pests reveal that pests strategically anticipate and exploit plant rhythms. For example, the cabbage looper (*Trichoplusia ni*), a generalist herbivore, shows rhythms in feeding, with peak feeding occurring during the latter part of the day (8). Conversely, cell-content feeders like spider mites (*Tetranychus urticae*) exploit a nighttime "lull" in jasmonate-induced defenses, causing more damage during the night (9). Given that aphids rely entirely on acquiring phloem sap from plants for their reproduction and survival, they likely need to anticipate, respond to, and counteract the challenges posed by daily rhythms in their hosts. Notably, green peach aphids (*Myzus persicae*) feeding on Arabidopsis plants exhibit peak honeydew droplet excretion during the day (10). These diurnal patterns in aphids extend beyond honeydew excretion, encompassing aspects such as locomotion, larviposition, sex hormone release, egg hatching, and feeding (11–15). While these studies have begun to broaden our understanding of aphid diurnal rhythms, our knowledge about how aphids regulate their rhythmic behaviors and interact with their hosts over daily cycles remains underexplored.

The high energy demand for aphid reproduction and the 'nitrogen and sugar barrier' in phloem sap necessitate aphids to feed almost incessantly from their host plants (16, 17). To facilitate this continuous feeding, aphids synthesize watery saliva in their salivary glands and secrete it into plant cells during feeding. This watery saliva comprises a complex blend of proteins with enzymatic activity, including cell-wall degrading enzymes, proteases, polyphenol oxidases, oxidoreductases, and peroxidases, as well as diverse calcium-binding proteins, and many others with unknown functions (18). Collectively termed effectors, these salivary proteins modify plant defense and physiology to facilitate aphid feeding, survival, and reproduction (19). With the advancement in omics technologies, numerous salivary effector candidates have been identified in several aphid species (20–22). An early and renowned example is C002, a protein

with an unknown function essential for continuous aphid feeding from sieve elements (23). Silencing C002 expression results in lethal outcomes in the pea aphid, *Acyrthosiphon pisum*, and diminished fecundity in the green peach aphid, *Myzus persicae* (24, 25). Despite the pivotal roles of salivary effectors in aphid colonization of host plants, knowledge about whether their expression or function undergo diurnal rhythms remains unknown.

Another consequence of relying solely on sugar-rich phloem sap is that aphids must process and excrete excess sugar to maintain an appropriate osmotic balance (17). Aphid osmoregulation involves physiological processes such as the breakdown of sucrose into glucose and fructose, their polymerization and expulsion as honeydew, and the rapid cycling of water between the midgut and hindgut (26, 27). Additionally, aphids feed during the night when phloem sugar content is lower (28) and occasionally drink dilute sap from the xylem, a behavior hypothesized to contribute to rehydration (29). At the molecular level, several genes involved in osmoregulation have been identified in aphids, and their silencing has been shown to elevate osmotic pressure in aphid hemolymph and impair performance (30–32). Previously, our group identified variation in the expression of osmoregulatory genes throughout a 24 h period in the bird cherry-oat aphid, *Rhopalosiphum padi* (28). Although diurnal fluctuation in phloem sap composition and its impact on aphid performance has been reported (33–36), an in-depth investigation into diurnal variation of aphid osmoregulation at the behavioral and molecular levels is currently lacking.

Here, we present findings that shed light on diurnal rhythmicity in feeding behavior and gene expression in *R. padi*, a serious pest of cereals worldwide and a major vector of the barley yellow dwarf virus (37). Our investigation reveals notable diurnal variation in honeydew excretion and specific feeding activities, particularly salivation into the phloem. A time-course transcriptomic experiment identified clusters of diurnally rhythmic genes with dynamic expression patterns enriched in diverse biological pathways. Putative salivary effectors were identified as diurnally rhythmic, with many showing peak expression during the night. By integrating behavioral and molecular findings, we unveil a substantial time-oriented role of osmoregulatory and salivary effector genes in aphids feeding on wheat plants. These findings provide novel insights into the diurnal regulation of aphid metabolism and behaviors, highlighting their crucial roles in colonizing host plants.

Results

Diurnal rhythmicity in *R. padi* feeding behaviors.

Diurnal variation of honeydew excretion in *R. padi* was investigated under a 12L:12D cycle for 48 h on wheat plants. Our study found that the number of honeydew droplets produced per aphid was higher during nighttime (12.09 ± 0.75, mean ± standard error of mean) as opposed to daytime (8.42 ± 0.57, $P = 0.0006$) (Fig. 1A). The experiment was repeated on an artificial diet to determine if the observed patterns were independent of plant-derived cues. Although fewer honeydew droplets were produced on diet overall, a higher number of honeydew droplets was

consistently produced per aphid on diet during the night (0.23 ± 0.05) compared to the day (0.09 ± 0.03, $P = 0.041$) (Fig. 1B).

The diurnal feeding behavior of *R. padi* was further elucidated using the electrical penetration graph (EPG) technique by measuring feeding at 4 h intervals over a 24 h period (12L:12D). Significant differences were observed in various aphid feeding activities over each timepoint (Dataset S1), including the phloem salivation (E1) phase. Adult *R. padi* spent the longest time in E1 between 12-16 zeitgeber time (zt, refers to an environmental agent or event that provides the stimulus to set or reset a biological clock) and the shortest time between 0-4zt, each of which represents the time period directly following the removal or introduction of the light cues, respectively (Fig. 1C). We also identified a diurnal rhythm in the total duration of E1 (COSINOR $P = 0.018$), with an acrophase (the estimated time in a rhythmic cycle when a peak or maximum value occurs) occurring at 9.8zt (Fig. 1C, *SI Appendix*, Table S1). Interestingly, despite the higher honeydew excretion at night (Fig 1A), the total time spent in phloem ingestion (E2 phase) did not differ over the 24 h period. No diurnal rhythm was detected for the E2 phase (Fig. 1D). Therefore, we hypothesize that the observed day-night variations in salivation and honeydew excretion are associated with diurnally regulated genes involved in the expression of salivary effectors and metabolic pathways linked to aphid feeding, such as osmoregulation.

Temporal gene expression patterns in *R. padi* reveal diurnal rhythmicity.

Temporal transcriptome profiles were collected from *R. padi* whole bodies over a 24 h period to identify diurnal rhythms in gene expression. A total of 49,486 transcripts were assembled with an average sequence length of 2,204 bp. The overall read mapping rate against the *R. padi* reference genome and Benchmarking Universal Single-Copy Orthologs (BUSCO) score for complete sequences were 97% and 99%, respectively (*SI Appendix*, Table S2). Of the total assembled transcripts, 4,460 (9.2%) showed significant diurnal rhythmicity over a 24 h period (Dataset S2). 2,913 and 1,547 rhythmic transcripts were identified to have acrophases during the day (0-12zt) and night (12-24zt), respectively. Most transcripts displayed acrophases between 4-8zt and 17-19zt, representing mid-day and midnight periods, respectively (Fig. 2A).

Soft-clustering analysis classified rhythmic transcripts into four discrete clusters (Fig 2B). Of the total rhythmic transcripts, 95% were clustered, with 1288, 431, 1143, and 1388 sequences assigned to clusters 1, 2, 3, and 4, respectively (Dataset S3). Most rhythmic transcripts in clusters 1 and 4 showed acrophases during the day at ~4-5zt and ~6-8zt. Cluster 2, containing the least number of transcripts (10% of clustered rhythmic transcripts), was represented by sequences with acrophases occurring during the late night-early morning transition (~21-1zt). Cluster 3 was mainly represented by transcripts with acrophases during the night at ~16-20zt.

Pathway enrichment analysis showed that cluster 1 was enriched in the pathways for the spliceosome, DNA replication, and basal transcription factors (Fig. 2C, Dataset S3), indicating the active regulation of mRNA and protein production during the day. Cluster 2 did not show significant pathway enrichment but exhibited significant gene ontology (GO) terms related to small molecule, lipid, and carbohydrate metabolic processes (*SI Appendix*, Fig. S1). Cluster 3

displayed enrichment in pathways associated with lysosome and various biochemical processes involved in starch, sugar, nitrogen, and amino acid metabolism, indicating higher night-time carbohydrate and amino acid metabolic activities in aphids. Cluster 4 was notably enriched in pathways related to purine metabolism, thiamine metabolism, and multiple pathways associated with human neurodegenerative diseases.

Silencing diurnally rhythmic osmoregulatory genes impacts aphid performance.

Osmoregulation is an important physiological activity to tolerate sugar-rich phloem sap during aphid feeding. Three osmoregulatory genes, *aquaporin 1* (AQP1) (31), *gut sucrase 1* (SUC1) (30, 38, 39), and *gut sugar transporter 4* (40), were previously reported to display diurnal patterns in *R. padi* (28). In our study, all three genes were confirmed to be diurnally rhythmic, with acrophases occurring at 15-22zt (Fig 2D-E, *SI Appendix*, Table S3). To determine whether the osmoregulatory genes contributed to diurnal variations in honeydew excretion, AQP1 and SUC1 were silenced by injecting aphids with dsRNA targeting each gene. A significant silencing of AQP1 and SUC1 was confirmed 24 hours post injection (hpi) (*SI Appendix*, Fig. S2 A-B) with a knockdown efficiency of 44% and 50%, respectively. Silencing AQP1 and SUC1 increased aphid mortality over time (Log-rank test $P = 0.0272$ and $P = 0.0003$, respectively), and reduced nymph production by 31% ($P = 0.044$) and 66% ($P < 0.0001$) at 96 hpi, respectively (Fig. 2F-G). Moreover, silencing the two genes markedly reduced honeydew excretion and abolished rhythms in the number of honeydew droplets produced by aphids between the day and night (Fig. 2H). This affirms their significant roles in the diurnal regulation of honeydew excretion and osmoregulation.

Diurnal rhythmicity in *R. padi* salivary effectors.

Given the observed diurnal rhythm in the E1 salivation phase, we sought to determine the presence of diurnal rhythms in the expression of aphid salivary effectors. Previously, 156 genes were identified as putative salivary effectors in *R. padi* (22). Our study retrieved 93% of putative effectors (145 genes represented by 264 transcripts) by searching all transcripts against the *R. padi* putative effector dataset (Dataset S4). Among them, 42 exhibited diurnal rhythmicity, with 28 exhibiting acrophases at 6-8zt during the day and 14 with acrophases at 18-19zt and 22-23zt at night (Fig. 3A, *SI Appendix*, Table S4).

The expression levels of these rhythmic putative effectors were further examined in *R. padi* heads compared to the bodies (body samples excluded tissue from heads and unborn nymphs). We confirmed that the expressions of all rhythmic putative effectors were significantly higher in the heads, except for the putative effector MSTRG.15390.2, which lacked assigned count values across head and body samples (*SI Appendix*, Fig. S3). Hierarchical clustering of the rhythmic putative effectors identified four main clades, each showing distinct times of peak expression (Fig. 3A). Transcripts in clades 1 and 2 peaked in expression at the transition from day to night and the early portion of mid-day, respectively. In contrast, transcripts within clade 3

exhibited peak expressions at the end of the night and early morning, while clade 4 consisted of transcripts with expression peaking towards the end of the night. Notably, 43% of rhythmic putative effectors with peak expressions occurring at 12-16zt in clade 1 and 4 coincided with the timing of increased E1 salivation, including a well-characterized salivary effector - C002 (AphidBase accession - g12266.t1).

GO enrichment analysis highlighted two significantly enriched terms for all putative effectors: extracellular region and chitin-binding (Fig. 3B). The former supports a secretory role for these effectors, and the latter implies their potential time-dependent functions in evading or interfering with chitin-triggered plant immunity (41, 42). These findings provide evidence of diurnal rhythms in salivary effector expression, with a subset peaking in expression at the same time as increased nighttime salivation. It also suggests that different blends of salivary effectors are secreted into the plants at different times of the day and represents the first report of diurnal rhythmicity in salivary effector gene expression in any aphid species.

Key salivary effectors identified for functional analysis.

To elucidate the functions of diurnally rhythmic salivary effectors in aphid-plant interactions, we selected C002 and a novel effector, E8696 (AphidBase accession - g8696.t1), based on their high amplitude values (i.e. half the difference between the highest and lowest points of a rhythmic cycle), positioning them among the top five compared to other rhythmic putative effectors (Fig. 4A, *SI Appendix*, Table S4). According to our soft-clustering analysis, C002 and E8696 were assigned to cluster 3 with membership scores of 0.895 and 0.979, respectively (Dataset S3). Their high membership scores designate them as core members within the cluster (43). Additionally, both genes also showed significantly higher expression in *R. padi* heads compared to bodies (Fig. 4B) and peaked in expression at 16zt (midnight) (Fig. 3C-D).

Sequence analysis revealed that E8696 encodes for a protein of unknown function with a predicted signal peptide (probability score: 0.953, cleavage site: amino acids 24-25) (*SI Appendix*, Fig. S4A). Phylogenetic analysis demonstrated the high conservation of this novel effector in aphid species, particularly in close relation to another cereal aphid, the corn leaf aphid, *R. maidis* (*SI Appendix*, Fig. S4B).

Disrupting diurnally rhythmic salivary effectors alters feeding dynamics and performance.

We further determined the role of C002 and E8696 in aphid feeding and performance through RNA interference. A significant knockdown of C002 and E8696 expression was confirmed at 24 hpi ($P < 0.05$), with significant C002 silencing sustaining until 48 hpi (Fig. S2C-D). Silencing efficiencies at 24 and 48 hpi were 37% and 27% for C002, and 29% and 26% for E8696, respectively. Silencing C002 reduced aphid survivorship (Log-rank test, $P = 0.0205$) and fecundity on wheat ($P < 0.0001$) (Fig. 4E-F), consistent with previous findings (23, 25, 44). Specifically, C002 silencing caused 29% aphid mortality and a 56% reduction in fecundity at 96 hpi compared to dsGFP control. Similarly, silencing of E8696 reduced aphid survivorship (Log-

rank test, $P = 0.0205$) and fecundity ($P < 0.0001$), causing a 79% mortality and 86% reduction in fecundity at 96 hpi. To uncouple the influence of plant-derived cues on aphid feeding, we also assessed aphid performance on artificial diets after silencing the two effector genes. In contrast to the results observed on wheat plants, silencing either gene did not affect aphid survivorship and fecundity (Fig. 4G-H).

On plants, silencing either effector gene reduced overall honeydew excretion, with only C002 silencing disrupting the diurnal rhythm in honeydew excretion (Fig. 4I). Nighttime honeydew excretion decreased by 1.7- and 1.4-fold compared to the day after silencing C002 (4.1 vs 2.4) and E8696 (4.1 vs 2.9). In contrast, silencing had no impact on honeydew excretion on artificial diets, and aphids consistently generated more honeydew droplets at night than during the day (Fig. 4J). Furthermore, we found no diurnal variation in nymph production post-silencing on both plant and diet (*SI Appendix*, Fig. S5). However, the overall number of nymphs was markedly lower compared to dsGFP controls on the plant ($P < 0.0001$), but not on the diet ($P = 0.8142$). These findings emphasize the time-oriented roles of these effectors in aphid feeding on plants.

Disturbed aphid feeding activities were also confirmed using EPG after silencing E8696. Aphids exhibited an increase in the average duration (total duration/number of each event) of the salivation phase (E1 phase, $P = 0.0071$), accompanied by a concurrent decrease in the phloem ingestion phase (E2 phase, $P = 0.0195$) (Fig. 4K, Dataset S5). These findings support our hypothesis that aphid feeding behavior and performance are tightly linked to and influenced by the diurnal expression of salivary effectors.

Discussion

The cyclical patterns of environmental and host-derived cues, dictated by the earth's light-dark cycle, significantly influence the physiology and behavior of organisms, including crop plants and their associated pests (1, 6). While studies have begun to show the prevalence of diurnal rhythms among aphid pests, critical knowledge gaps persist regarding how these rhythms facilitate interactions between aphids and their hosts. Our study aimed to fill these knowledge gaps by assessing diurnal rhythms in behavior and gene expression in the bird-cherry oat aphid (*R. padi*), a major pest on cereals worldwide. We further characterized the impact of diurnally rhythmic osmoregulatory and salivary effector genes on *R. padi* behavior and performance.

Here, our study found that aphids exhibited diurnal rhythms in feeding behaviors, particularly in the duration of phloem salivation (E1 phase) and various probing activities. The pronounced nighttime increase in phloem salivation suggests that aphids may be responding to changes in plant defenses or phloem quality, which are known to exhibit diurnal variation in numerous plant species (45–47). Our study also found that the duration of phloem and xylem sap ingestion (E2 and G phases, respectively) showed no significant differences over a 24 h cycle. The desire for aphids to quickly reach and remain in the E2 phase regardless of timepoint, coupled with the strong diurnal variation in honeydew excretion, might suggest that aphids do not modulate feeding behavior as a tool for osmoregulation but rather rely on metabolic

mechanisms to process and excrete excess sugar. The low occurrence and the lack of diurnal variation in the G phase further suggest that excretion methods might make up for the majority of aphid osmoregulatory function across a 24 h period, with xylem ingestion only occurring in aphids that are severely dehydrated. These findings align with the nutritional and reproductive strategy of aphids, emphasizing the importance of acquiring sufficient sugar and amino acids for population growth and survival.

Remarkably, *R. padi* excreted more honeydew droplets during the nighttime on wheat plants, contrary to previously documented patterns (10, 11). This divergence in honeydew excretion patterns suggests species-level differences in aphid osmoregulatory rhythms, potentially reflecting variance in phloem quality across host species. Notably, the persistence of honeydew excretion patterns in *R. padi* on artificial diets, devoid of plant-derived cues, suggests an internal circadian clock-driven mechanism. However, it should be noted that these experiments were only conducted in the absence of plant-derived cues. To determine the involvement of the circadian clock in regulating the rhythms uncovered in our study, all cues, including plant, light, and temperature, would need to be removed.

Our time-course transcriptomic analysis revealed a comprehensive view of diurnal gene expression in *R. padi*, revealing approximately 9% of total assembled transcripts display diurnal rhythms. Most transcripts display acrophases 6 h after the start and end of the light cue (noon or 4zt and midnight or 16zt, respectively). The bimodal pattern of transcript acrophases could be evidence that noon and midnight are periods of high activity in aphids, with multiple physiological and behavioral processes potentially occurring at or around these times. Comparisons with studies in Drosophila and the malaria mosquito (*Anopheles gambiae*), estimating rhythmic expression in 10% and 15.8% of genes linked to various biological functions [45–48], support the notion of diurnal regulation in aphids. The expression profiles of clustered rhythmic transcripts, with each gene cluster exhibiting peak expression at specific times of the day, point to a transcriptional control mechanism, potentially orchestrated by the aphid's circadian clock. A more in-depth investigation is warranted to determine the role of circadian clock regulation in gene expression, particularly after eliminating the influence of host and environmental cues (2). Our enrichment analysis highlighted the functional diversity within diurnally rhythmic gene clusters, particularly in metabolic activities between the day and night. Notably, rhythmic transcripts in night-peaking clusters 2 and 3 were predominantly enriched in pathways related to the metabolism of carbohydrates, amino acids, lipids, and other small molecules. The heightened metabolic pathways at night align with our observed diurnal rhythms in honeydew excretion, suggesting a correlation between these metabolic processes and the regulation of honeydew excretion.

Previous research has demonstrated that silencing AQP1 and SUC1 in *M. persicae* led to elevated hemolymph osmotic pressure, accompanied by a decrease in aphid weight and fecundity (32). In our study, a parallel decline in aphid performance was observed, where the knockdown of AQP1 and SUC1 in *R. padi* resulted in increased mortality and diminished fecundity. Notably, these two genes exhibited a pronounced diurnal rhythm, indicating that osmoregulation experiences peak activity at specific times of day, potentially corresponding to changes in

phloem sap quality. Another aspect of osmoregulation is the excretion of oligosaccharides in the form of honeydew (26). The overall reduction in quantity and the abolition of rhythms in honeydew excretion upon the silencing of AQP1 and SUC1 suggests a pivotal role for these genes and their diurnal variation in shaping honeydew excretion behaviors of aphids.

Our study found a notable increase in the salivation (E1) phase into the phloem at the start of the night. In contrast, other important feeding behaviors, such as phloem sap ingestion (E2 phase), remained uniform throughout the 24 h period. This suggests that while aphids spend similar durations feeding from the phloem during both the day and night, specific time-of-day-based changes in the host plant may necessitate aphids to modulate host plant responses through salivation and the introduction of specific effectors. The expression patterns of several salivary effector genes also exhibited diurnal rhythm, indicating that variations in the effector blends introduced into the plant may play a role in modulating time-of-day specific host plant responses. Silencing the diurnally rhythmic effectors C002 and E8696 induced high mortality and reduced fecundity in *R. padi* feeding on wheat. However, this trend was absent on artificial diets, underscoring the crucial role of these effectors in facilitating the interaction between the plant and the aphid. Notably, silencing these two effectors also resulted in a more pronounced reduction in nighttime honeydew excretion compared to the day on wheat plants, while having no impact on diurnal honeydew excretion on diets. This may suggest their crucial roles in optimizing aphid feeding strategies, potentially enhancing their adaptation to the host plant's physiological changes during the night. Further experiments conducted in the absence of time-of-day cues are necessary to discern whether the rhythmic activity of these effectors is driven by circadian clock regulation in the aphid, fluctuations in phloem sap quality or plant defenses, merely a response to environmental changes across the diurnal period, or some combination of each.

In summary, our findings demonstrate substantial alterations in the behavior and physiology of an important plant pest throughout the day. Exploring the daily variations in aphids offers a new lens through which to understand the molecular, behavioral, and ecological factors shaping aphid-plant interactions. Furthermore, the knowledge gained by these experiments has the potential to guide the development of innovative pest control strategies. By capitalizing on the daily rhythms in moments of strengths and vulnerabilities in crop plants and their pests, we envision an era of "chronoculture," where harnessing circadian rhythms in plants and their pests contributes to enhancing crop yield and sustainability (6).

Materials and Methods

Aphid colonies and plant growth conditions

A colony of bird cherry-oat aphids (*Rhopalosiphum padi*) was initiated with aphids collected from greenhouses at the Plant Growth Facility at Colorado State University, Fort Collins, and has been maintained in the laboratory since 2019. *R. padi* was reared on three-week-old barley seedlings (*Hordeum vulgare* var. AC Metcalfe). Colony plants were replenished every two to three weeks or when overcrowding occurred. All plants were grown in PRO-MIX BX General

Purpose Growing Medium (Premier Tech Horticulture, Quakertown, PA) in mylar plant growth tents at 60-70% relative humidity, temperature of 24 ± 1ºC and maintained under a short-day photoperiod of 12L:12D at photosynthetically active radiation (PAR) of 460 µmol/m^2/s. Plants were watered three times per week and fertilized with Miracle Gro® (Scott's Co. LLC, Marysville, OH, USA) once a week. All experiments were performed on wheat (*Triticum aestivum* var. Chinese Spring) plants that were 14-21 days old or at the two-leaf stage (Zadoks stage, Z1.2) (48).

Aphid age synchronization

All experiments used age-synchronized aphids to limit any age-related effects on aphid behaviors or gene expression (49). Briefly, adult aphids from the colony were placed into a feeding chamber containing the second and third leaves of a two-week-old wheat plant. The feeding chamber was made from a 50-ml falcon tube with the bottom side cut open and the lid modified for ventilation using aphid-proof mesh. Leaves were inserted into the tube from the bottom opening and sealed with a cotton ball. After 48 h, adult aphids were removed, and nymphs were allowed to develop to adulthood on the plant for five days.

Aphid feeding assay on wheat and artificial diet

Five age-synchronized aphids were placed into a 55 mm Petri dish (V.W.R., Radnor, PA) modified to contain leaf 2 of a wheat plant (Z1.2) (*SI Appendix*, Fig. S6). Nymph count and honeydew droplet production were recorded at the onset of day and night over 48 h, adhering to a 12L:12D photoperiod. Discrete honeydew droplets were counted instead of using a staining and area calculation method. This choice was made because droplets exhibit uniform size and were easily visible to the naked eye. However, their translucent color made capturing them in photographs and measuring the area challenging. After each measurement, nymphs were carefully removed, and the honeydew-soiled lid was replaced with a fresh one. Concurrently, feeding assays were conducted using an artificial diet designed for *R. padi* (50). An artificial feeding chamber was constructed under sterile conditions and consisted of 58 mm Petri-dish lids with Parafilm sachets containing 1.5 ml of diet. Five age-synchronized aphids were placed into the artificial feeding chamber (*SI Appendix*, Fig. S6) and the number of nymphs and honeydew droplets were measured as described above. Both experiments were independently conducted on two occasions, with five replicates on each occasion. Statistical differences between treatments were tested using the Mann-Whitney test ($P < 0.05$).

Electrical penetration graph

Adult *R. padi* feeding behavior was recorded on wheat seedlings (Z1.2) using the electrical penetration graph (EPG) (51) technique on a GIGA 8 complete system (EPG systems, Wageningen, Netherlands). The recordings were performed every 4 h over a 24 h period starting at 0zt (a total of six time periods). Age-synchronized adult *R. padi* were starved for 1 h before wiring. Next, plant electrodes were inserted into the soil, and insect probes adjusted to ensure contact between the plant surface and the insect. Aphids were only allowed to feed from the leaf 2 and only one aphid was recorded per plant. For recordings that were initiated in the night or scotophase (0zt, 16zt, and 20zt), all setup was performed with a red LED headlight (Energizer).

The 0zt timepoint was set up in dark conditions while feeding behavior was recorded in light. The 12zt timepoint was set up in light conditions, with feeding behavior recorded in darkness. Photoperiod and the temperatures during the day and night were the same as what was used for plant and aphid growing conditions. Both plants and aphids were discarded after each 4 h recording. The analysis of each feeding experiment aimed to determine the time allocation across four primary phases: the pathway or probing phase (C), non-probing phase (NP), salivation phase (E1), phloem sap ingestion phase (E2), and xylem phase (G). Additionally, many EPG parameters that characterize aphid probing and ingestion (52) were determined to develop a comprehensive picture of aphid feeding over a 24 h period. EPG parameters were calculated using the discoEPG package integrated into the web-based R/shiny app (https://nalamlab.shinyapps.io/test/). There were 25 replicates for 0zt, 21 replicates for 4zt, 26 replicates for 8zt, 23 replicates for 12zt, 29 replicates for 16zt, and 16 replicates for 20zt. Recordings without feeding or probing events and those with more than 70% of time spent in NP + derailed stylet phase (F) + G were excluded from analysis. Statistical differences between the six time periods of each EPG phase were tested using the Kruskal–Wallis test with Bonferroni adjustment for *p*-values (adjusted $P < 0.05$). Rhythmicity of EPG phases was determined with the average total duration (minutes) of each recorded waveform across the different periods using a COSINOR-based oscillation detection method in DiscoRhythm v1.2.1 (53). EPG phases were considered significant rhythmic if their *p*-values were less than 0.05, and their corresponding oscillation parameters were estimated.

Sample collection, RNA isolation, library preparation, and RNA Sequencing

A cohort of adult *R. padi* (~100) were evenly distributed on wheat plants (Z1.2). The adults were removed after 24 h, and the nymphs were allowed to develop to adulthood for six days. These age-synchronized *R. padi* adults were collected from wheat plants every four hours over a 24 h period (12L:12D), starting at 0zt (when the lights were turned on) and ending at 20zt (*SI Appendix*, Fig. S7). A pool of 30 apterous aphids was collected per sample and extracted for total RNA using the Quick-RNA Miniprep Kit (Zymo Research, Irvine, CA) according to the manufacturer's instructions. This time-course RNA-Seq experiment comprised three biological replicates of aphid samples per time point. RNA quality and concentration were measured using a Nanodrop spectrophotometer (Thermo Scientific, Waltham, MA) and Agilent 2100 Bioanalyzer (Santa Clara, CA). Aphid RNA samples were sent to Novogene Corporation Inc. (Sacramento, CA) for cDNA library construction and RNA sequencing. The poly(A) mRNA-enriched libraries were constructed using NEBNext® Ultra™ II RNA Library Prep Kit (New England BioLabs, Ipswich, MA). Paired-end sequencing (2×150 bp) was conducted with the Illumina HiSeq 2000 platform. The raw sequencing reads have been deposited in the NCBI SRA database under the BioProject accession PRJNA979927.

Genome-guided transcriptome assembly and read mapping

Raw sequence reads were trimmed for adapters and quality using fastp v0.23.3(54). The reads with a Phred score less than 25 and lengths shorter than 100 bp were discarded. The high-quality reads from each library were mapped against the *R. padi* reference genome (v2.0) available on AphidBase (https://bipaa.genouest.org/is/aphidbase/) using Hisat2 v2.2.1. The mapped reads

were assembled into transcripts using Stringtie v2.2.1. The assemblies from all 18 libraries were further merged to generate a reference transcriptome using the Stringtie -merge function (55). Reads representing each sampling timepoint were mapped back to this reference transcriptome to quantify the gene expression using Salmon v1.9.0 (56).

Identification and clustering of diurnal rhythmic transcripts

The non-random rhythmicity of *R. padi* genes was determined with a COSINOR-based oscillation detection method in DiscoRhythm v1.2.1 (53). The temporal expression data of all transcripts identified in the whole-body *R. padi* (48,690) were utilized for detecting rhythmic signals. The expression data was filtered for constant or missing values (>25%) across the samples, resulting in 38,871 transcripts. Rhythm detection and estimation of oscillation parameters were performed as previously outlined. Soft clustering of all rhythmic sequences was carried out to identify major temporal patterns of rhythmic expression using the R package, mFuzz v2.56.0 (43). Membership values ranging from 0 to 1 were assigned to clustered transcripts. Sequences with a membership value > 0.7 were considered core members of each cluster (57).

Gene ontology and pathway enrichment analyses

All clustered sequences of rhythmic transcripts in *R. padi* were blastx-searched against the NCBI non-redundant (nr) protein database using OmicsBox v2.2 with an E-value cut-off of 1e-5 (58). Sequences with assigned gene ontology (GO) terms were categorized into biological process, molecular function, and cellular component categories. Further, these clustered sequences were annotated for the Kyoto Encyclopedia of Genes and Genomes (KEGG) orthologs and linked to corresponding KEGG reference pathways. GO and KEGG pathway enrichment analyses were performed for rhythmic transcripts within each of the four gene clusters and the rhythmic putative salivary effector transcripts using a two-tailed Fisher's exact test with an FDR cut-off of 0.05 in OmicsBox (58). The entire *R. padi* transcriptome was used as the background gene set for both enrichment analyses.

Identification of diurnally rhythmic osmoregulatory and putative salivary effector genes

Osmoregulatory genes in *R. padi* were identified as described previously (28). Briefly, homologs for these genes were identified by querying *Acyrthosiphon pisum* gene sequences with the *R. padi* reference genome (v2.0) on AphidBase (59) using Blastp. Further validation involved searching protein sequences with DeepTMHMM (60) and SMART (61) to determine the presence of sequence features. All *R. padi* transcripts were searched against the curated putative salivary effector database for *R. padi* (22) using Blast+ v2.13.0 with an E-value cut-off of 1e-5. Stringent criteria were applied, with thresholds set at 80% for identity and 50% for coverage to identify putative salivary effectors. To quantify tissue-specific expression of these rhythmic putative effectors, RNA-Seq reads of *R. padi* heads and bodies (not including heads and nymphs) were retrieved through the European Nucleotide Archive under the project accession number of PRJEB9912 (22). Sample accessions for head and body datasets are as follows: SAMEA3505144, SAMEA3505145, SAMEA3505146, SAMEA3505147, SAMEA3505148, SAMEA3505149. Reads were trimmed for adapters and quality and mapped against the

previously assembled *R. padi* reference transcriptome using the abovementioned pipeline. The diurnal rhythmicity of identified osmoregulatory and putative effector sequences was tested using the COSINOR model described above.

Sequence and phylogenetic analyses of a novel putative salivary effector

The full-length coding sequence of E8696 was queried against the NCBI nr protein database with organism specified as aphids. There were 25 sequence hits in the database for E8696. The top hit of each aphid species was retrieved and used for sequence analysis (*SI Appendix*, Table S5). Signal peptide, transmembrane helix, and other conserved domains were analyzed using SignalP v6.0, DeepTMHMM, and NCBI Conserved Domain Search (62–64). Multiple sequence alignments were performed using MUSCLE, and the phylogenetic trees were built using the maximum likelihood method with GTR+G as the best-fit substitution model in MEGA 11 software (65). Node support rates were assessed with 1,000 bootstrap replicates.

Design and synthesis of double-stranded RNAs

Sequence analysis was performed on the four target genes: AQP1, SUC1, C002, and E8696. The open reading frames and potential conserved domains were identified using the NCBI ORFfinder and Conserved Domain Search tools (64). The nucleotide sequence of each gene was evaluated to identify optimal target regions of double-stranded RNA (dsRNA). Corresponding primers were designed using the E-RNAi web tool (66) (*SI Appendix*, Table S6). The specificity of dsRNA primers was confirmed through a search against the NCBI *R. padi* nr database using the Primer-BLAST tool and in PCR, followed by agarose gel electrophoresis. For dsRNA synthesis, total RNA was extracted from a pool of ~30 *R. padi* containing all five developmental stages using Direct-zol RNA Microprep Kit (Zymo Research, Irvine, CA) according to the manufacturer's protocol. cDNA was synthesized from 1 µg of DNase-treated RNA using the Verso cDNA Synthesis Kit (Thermo Scientific, Waltham, MA). The dsRNA sequence region of each gene was amplified with the gene-specific primer pair using Q5 high-fidelity PCR (New England BioLabs, Ipswich, MA). The sense and antisense dsRNA sequence fragments conjugated with the T7 promoter sequence were amplified separately using the previous PCR amplicons as templates. All PCR products were confirmed for unique and accurate amplification in agarose gels and purified using GeneJET PCR Purification Kit (Thermo Scientific, Waltham, MA). dsRNA was synthesized with 1 µg of purified PCR products using the T7 RiboMAX Express RNAi System, according to the manufacturer's instructions (Promega, Madison, WI). dsRNA targeting the green fluorescent protein (GFP) gene was synthesized following the protocol described above and used as a negative control. The quantity and integrity of dsRNA were measured by Nanodrop spectrophotometer (Thermo Scientific, Waltham, MA) and agarose gel electrophoresis.

Microinjection of aphids with dsRNA

Injection needles (Drummond Scientific Co., Broomall, PA) were produced by pulling with a P-1000 micropipette puller (Sutter Instrument Co. Novato, CA) using optimized settings: heat=500, pull=100, velocity=40, delay=100, pressure=500, and ramp=493. The glass needle, filled with 5 µl of dsRNA, was assembled onto a Nanoject III microinjector (Drummond

Scientific Co., Broomall, PA). Age-synchronized aphids were immobilized on a sticky tape strip (ventral side up) and injected with 180 ng of dsRNA (40 nl of 4.5 µg/µl) through the flexible membrane between the coxa of the hind leg and thorax. Immediately after injection, aphids were carefully detached from the tape using a wet paintbrush and transferred to a feeding chamber containing wheat leaves. The injection process was repeated until the desired number of aphids was achieved. The same procedure was applied to the other dsRNA treatment groups. The injected aphids were incubated at 25°C, 12L:12D photoperiod. Each experiment was independently replicated three times.

Gene silencing in aphids

Five aphids, collected at 24- and 48-hour post-injection from three biological replicates, were subjected to RNA extraction using the Direct-zol® RNA Microprep Kit as described above. cDNA was synthesized from 500 ng of RNA and diluted 4-fold with nuclease-free water. Quantitative PCR (qPCR) was employed to measure the expression of the target gene and the housekeeping gene, Actin (AphidBase accession - g9633.t1). Gene-specific qPCR primers were designed using the NCBI Primer-Blast tool (*SI Appendix*, Table S6). A duplicate of 10 µl SYBR Green Supermix reaction (Bio-Rad, Hercules, CA) containing 2 µl of cDNA template was prepared and analyzed using CFX Connect Real-Time instrument (BioRad) with the following thermocycling conditions: 95°C for 30s, followed by 40 cycles of 95°C for 10s, 55°C for 30s, 72°C for 30s, with a final melt curve of 95°C for 30s, 65°C for 5s increasing to a final temperature of 95°C. The relative normalized expression of each target gene was estimated using the Pfaffl method (67). Statistical differences in gene expression between treatments at each time point were assessed using a two-tailed Welch's t-test ($P < 0.05$).

Aphid performance and feeding assays on wheat and artificial diet after gene knockdown

RNA interference (RNAi) was used to functionally characterize two osmoregulatory genes, aquaporin 1 (AQP1) and gut sucrase 1 (SUC1). Nine aphids injected with dsRNA AQP1 (dsAQP1) or dsRNA SUC1 (dsSUC1) were placed into a feeding chamber containing wheat leaves (*SI Appendix*, Fig. S8A). Aphid mortality and fecundity (cumulative nymph count) were recorded every 24 h for 4 days. Aphids injected with dsRNA GFP (dsGFP) were the negative control. The number of honeydew droplets produced by five dsRNA-injected aphids on wheat plants were recorded at the beginning of the day and night for 4 days under a short-day photoperiod as described previously (*SI Appendix*, Fig. S6). Similar experimental setups were replicated for two target salivary effector genes, C002 and E8696, to measure aphid mortality and fecundity. Additionally, five aphids injected with dsRNA C002 (dsC002) or dsRNA E8696 (dsE8696) were placed on an artificial diet (*SI Appendix*, Fig. S8B) and monitored for mortality and fecundity every 24 h for 4 days. To further assess daily changes in honeydew excretion and fecundity, five aphids after 24 h post-injection with dsC002 or dsE8696 were placed on a wheat leaf or artificial diet. The numbers of honeydew droplets and nymphs were recorded as previously described (*SI Appendix*, Fig. S6). All experiments were independently repeated three times. Kaplan-Meier survival curves were generated for dsRNA-injected aphids and compared for statistical differences by the Mantel-Cox log-rank test with Benjamini–Hochberg false discovery rate adjusted *p*-values (adjusted $P < 0.05$) using the 'survminer' R package. The

statistical difference in the nymph count of dsRNA-injected aphids was determined using a general linear model for repeated measures with Tukey's multiple comparisons (adjusted $P < 0.05$). The normality of input data was confirmed using the Shapiro-Wilk test ($P > 0.05$). Statistical differences in honeydew and nymph productions between treatments were tested using the Mann-Whitney test ($P < 0.05$) and Kruskal-Wallis test, followed by Dunn's multiple comparison tests (adjusted $P < 0.05$).

Electrical penetration graph after silencing E8696

Age-synchronized *R. padi* were injected with dsE8696 or dsGFP as described above. Twenty-four hours post microinjection, individual aphids were wired and subjected to EPG recording to document their feeding activities on wheat plants (Z1.2) as described previously. Recordings started at 0zt, and feeding behavior was recorded for 8h for each aphid. The experiment included 13 replicates for dsE8696 and 15 replicates for the dsGFP control group. EPG parameters were calculated as previously described, and statistical differences between the two treatments were tested using the Mann-Whitney test ($P < 0.05$).

Author Contributions: J.H., D.K., V.T, and V.J.N designed the research; J.H., D.K., Y.G., and M.C. performed the research; J.H., D.K., M.C., Y.G., V.T, and V.J.N analyzed the data; and J.H., D.K., V.T, and V.J.N wrote the paper.

Competing Interest Statement: The authors declare no competing interest.

Acknowledgments

We thank Joely Corrales for her assistance with planting and aphid synchronization. Drs. Jan Leach, Micky Eubanks, and Punya Nachappa for internal review of the manuscript. The project was funded by the United States – Israel Binational Science Foundation grant (Proposal#202181, PIs Vered Tzin and Vamsi Nalam), Research Capacity Fund (COL0044) from NIFA and start-up funds from Colorado State University to Vamsi Nalam.

References

1. U. Bhadra, N. Thakkar, P. Das, M. Pal Bhadra, Evolution of circadian rhythms: from bacteria to human. *Sleep Med* **35**, 49–61 (2017).

2. M. H. Vitaterna, J. S. Takahashi, F. W. Turek, Overview of Circadian Rhythms. *Alcohol Research & Health* **25**, 85 (2001).

3. K. Beer, C. Helfrich-Förster, Model and Non-model Insects in Chronobiology. *Front Behav Neurosci* **14**, 221 (2020).

4. S. S. C. Rund, A. J. O'Donnell, J. E. Gentile, S. E. Reece, Daily rhythms in mosquitoes and their consequences for malaria transmission. *Insects* **7** (2016).

5. C. T. Hotta, From crops to shops: How agriculture can use circadian clocks. *J Exp Bot* **72** (2021).

6. G. Steed, D. C. Ramirez, M. A. Hannah, A. A. R. Webb, Chronoculture, harnessing the circadian clock to improve crop yield and sustainability. *Science (1979)* **372** (2021).

7. C. A. Dedryver, A. le Ralec, F. Fabre, The conflicting relationships between aphids and men: A review of aphid damage and control strategies. *C R Biol* **333**, 539–553 (2010).

8. D. Goodspeed, E. W. Chehab, A. Min-Venditti, J. Braam, M. F. Covington, *Arabidopsis* synchronizes jasmonate-mediated defense with insect circadian behavior. *Proc Natl Acad Sci U S A* **109**, 4674–4677 (2012).

9. J. Liu, *et al.*, Spider Mites Cause More Damage to Tomato in the Dark When Induced Defenses Are Lower. *J Chem Ecol* **46** (2020).

10. J. Lei, *et al.*, CIRCADIAN CLOCK-ASSOCIATED1 controls resistance to aphids by altering indole glucosinolate production. *Plant Physiol* **181**, 1344–1359 (2019).

11. K. Beer, J. Joschinski, A. Arrazola Sastre, J. Krauss, C. Helfrich-Förster, A damping circadian clock drives weak oscillations in metabolism and locomotor activity of aphids (*Acyrthosiphon pisum*). *Scientific Reports 2017 7:1* **7**, 1–9 (2017).

12. J. Eisenbach, T. E. Mittler, An aphid circadian rhythm: Factors affecting the release of sex pheromone by oviparae of the greenbug, *Schizaphis graminum*. *J Insect Physiol* **26**, 511–515 (1980).

13. C. J. Hodgson, I. R. Lane, Some effects of photoperiod on larviposition and fresh weight-gain in *Myzus persicae*. *Physiol Entomol* **6** (1981).

14. J. Joschinski, K. Beer, C. Helfrich-Förster, J. Krauss, Pea aphids (Hemiptera: Aphididae) have diurnal rhythms when raised independently of a host plant. *Journal of Insect Science* **16** (2016).

15. N. Matsuda, Hatching rhythm and clock gene expression in the egg of the pea aphid, *Acyrthosiphon pisum*. *J Insect Physiol* **145** (2023).

16. A. E. Douglas, The Nutritional Physiology of Aphids. *Adv In Insect Phys* **31** (2003).

17. A. E. Douglas, Phloem-sap feeding by animals: Problems and solutions in *Journal of Experimental Botany*, (2006).

18. A. J. E. van Bel, T. Will, Functional evaluation of proteins in watery and gel saliva of aphids. *Front Plant Sci* **7**, 1840 (2016).

19. H. A. Mondal, Aphid saliva: a powerful recipe for modulating host resistance towards aphid clonal propagation. *Arthropod Plant Interact* **14**, 547–558 (2020).

20. J. I. B. Bos, *et al.*, A functional genomics approach identifies candidate effectors from the aphid species *Myzus persicae* (green peach aphid). *PLoS Genet* **6** (2010).

21. J. C. Carolan, *et al.*, Predicted effector molecules in the salivary secretome of the pea aphid (*Acyrthosiphon pisum*): A dual transcriptomic/proteomic approach. *J Proteome Res* **10**, 1505–1518 (2011).

22. P. Thorpe, P. J. A. Cock, J. Bos, Comparative transcriptomics and proteomics of three different aphid species identifies core and diverse effector sets. *BMC Genomics* **17** (2016).

23. N. S. Mutti, *et al.*, A protein from the salivary glands of the pea aphid, *Acyrthosiphon pisum*, is essential in feeding on a host plant. *Proc Natl Acad Sci U S A* **105**, 9965 (2008).

24. N. S. Mutti, Y. Park, J. C. Reese, G. R. Reeck, RNAi knockdown of a salivary transcript leading to lethality in the pea aphid, *Acyrthosiphon pisum*. *Journal of Insect Science* **6** (2006).

25. M. Pitino, A. D. Coleman, M. E. Maffei, C. J. Ridout, S. A. Hogenhout, Silencing of aphid genes by dsRNA feeding from plants. *PLoS One* **6** (2011).

26. T. L. Wilkinson, D. A. Ashford, J. Pritchard, A. E. Douglas, Honeydew Sugars and Osmoregulation in the Pea Aphid *Acyrthosiphon pisum*. *Journal of Experimental Biology* **200**, 2137–2143 (1997).

27. D. B. Fisher, J. P. Wright, T. E. Mittler, Osmoregulation by the aphid *Myzus persicae*: A physiological role for honeydew oligosaccharides. *J Insect Physiol* **30** (1984).

28. V. Nalam, *et al.*, Diurnal feeding as a potential mechanism of osmoregulation in aphids. *Insect Sci* **28**, 521–532 (2021).

29. N. J. Spiller, L. Koenders, W. F. Tjallingii, Xylem ingestion by aphids – a strategy for maintaining water balance. *Entomol Exp Appl* **55** (1990).

30. A. J. Karley, D. A. Ashford, L. M. Minto, J. Pritchard, A. E. Douglas, The significance of gut sucrase activity for osmoregulation in the pea aphid, *Acyrthosiphon pisum*. *J Insect Physiol* **51**, 1313–1319 (2005).

31. A. J. Shakesby, *et al.*, A water-specific aquaporin involved in aphid osmoregulation. *Insect Biochem Mol Biol* **39**, 1–10 (2009).

32. V. Tzin, *et al.*, RNA interference against gut osmoregulatory genes in phloem-feeding insects. *J Insect Physiol* **79** (2015).

33. D. C. Cull, H. F. V. Emden, The effect on *Aphis fabae* of diel changes in their food quality. *Physiol Entomol* **2** (1977).

34. S. Gattolin, *et al.*, A diurnal component to the variation in sieve tube amino acid content in wheat. *Plant Physiol* **147** (2008).

35. S. K. Gomez, D. M. Oosterhuis, D. L. Hendrix, D. R. Johnson, D. C. Steinkraus, Diurnal pattern of aphid feeding and its effect on cotton leaf physiology. *Environ Exp Bot* **55** (2006).

36. J. Kallarackal, S. N. Bauer, H. Nowak, M. R. Hajirezaei, E. Komor, Diurnal changes in assimilate concentrations and fluxes in the phloem of castor bean (*Ricinus communis* L.) and tansy (*Tanacetum vulgare* L.). *Planta* **236** (2012).

37. K. J. Finlay, J. E. Luck, Response of the bird cherry-oat aphid (*Rhopalosiphum padi*) to climate change in relation to its pest status, vectoring potential and function in a crop–vector–virus pathosystem. *Agric Ecosyst Environ* **144**, 405–421 (2011).

38. P. T. Cristofoletti, A. F. Ribeiro, C. Deraison, Y. Rahbé, W. R. Terra, Midgut adaptation and digestive enzyme distribution in a phloem feeding insect, the pea aphid *Acyrthosiphon pisum*. *J Insect Physiol* **49**, 11–24 (2003).

39. D. R. G. Price, *et al.*, Molecular characterisation of a candidate gut sucrase in the pea aphid, *Acyrthosiphon pisum*. *Insect Biochem Mol Biol* **37**, 307–317 (2007).

40. D. R. G. Price, J. A. Gatehouse, Genome-wide annotation and functional identification of aphid GLUT-like sugar transporters. *BMC Genomics* **15** (2014).

41. T. Y. Toruño, I. Stergiopoulos, G. Coaker, Plant-Pathogen Effectors: Cellular Probes Interfering with Plant Defenses in Spatial and Temporal Manners. *Annu Rev Phytopathol* **54** (2016).

42. A. D. Yates-Stewart, *et al.*, Soybean aphids adapted to host-plant resistance by down regulating putative effectors and up regulating transposable elements. *Insect Biochem Mol Biol* **121** (2020).

43. L. Kumar, M. E. Futschik, Mfuzz: A software package for soft clustering of microarray data. *Bioinformation* **2** (2007).

44. C. Escudero-Martinez, *et al.*, An aphid effector promotes barley susceptibility through suppression of defence gene expression. *J Exp Bot* **71**, 2796 (2020).

45. D. Goodspeed, E. W. Chehab, A. Min-Venditti, J. Braam, M. F. Covington, *Arabidopsis* synchronizes jasmonate-mediated defense with insect circadian behavior. *Proc Natl Acad Sci U S A* **109**, 4674–4677 (2012).

46. H. Winter, G. Lohaus, H. W. Heldt, Phloem Transport of Amino Acids in Relation to their Cytosolic Levels in Barley Leaves. *Plant Physiol* **99**, 996 (1992).

47. S. Gattolin, *et al.*, A Diurnal Component to the Variation in Sieve Tube Amino Acid Content in Wheat. *Plant Physiol* **147**, 912 (2008).

48. J. C. Zadoks, T. T. Chang, C. F. Konzak, A decimal code for the growth stages of cereals. *Weed Res* **14** (1974).

49. Y. Li, C. B. Hill, G. L. Hartman, Effect of three resistant soybean genotypes on the fecundity, mortality, and maturation of soybean aphid (Homoptera: Aphididae). *J Econ Entomol* **97** (2004).

50. J. L. Auclair, Feeding and Nutrition of the Pea Aphid, Acyrthosiphon pisum (Homoptera: Aphidae), on Chemically Defined Diets of Various pH and Nutrient Levels. *Ann Entomol Soc Am* **58**, 855–875 (1965).

51. W. F. Tjallingii, T. H. Esch, Fine structure of aphid stylet routes in plant tissues in correlation with EPG signals. *Physiol Entomol* **18** (1993).

52. E. Sarria, M. Cid, E. Garzo, A. Fereres, Excel Workbook for automatic parameter calculation of EPG data. *Comput Electron Agric* **67**, 35–42 (2009).

53. M. Carlucci, *et al.*, DiscoRhythm: An easy-to-use web application and R package for discovering rhythmicity. *Bioinformatics* **36** (2020).

54. S. Chen, Y. Zhou, Y. Chen, J. Gu, Fastp: An ultra-fast all-in-one FASTQ preprocessor in *Bioinformatics*, (2018).

55. M. Pertea, D. Kim, G. M. Pertea, J. T. Leek, S. L. Salzberg, Transcript-level expression analysis of RNA-seq experiments with HISAT, StringTie and Ballgown. *Nature Protocols 2016 11:9* **11**, 1650–1667 (2016).

56. R. Patro, G. Duggal, M. I. Love, R. A. Irizarry, C. Kingsford, Salmon provides fast and bias-aware quantification of transcript expression. *Nature Methods 2017 14:4* **14**, 417–419 (2017).

57. M. E. Futschik, B. Carlisle, Noise-robust soft clustering of gene expression time-course data. *J Bioinform Comput Biol* **3** (2005).

58. S. Götz, *et al.*, High-throughput functional annotation and data mining with the Blast2GO suite. *Nucleic Acids Res* **36** (2008).

59. J. P. Gauthier, F. Legeai, A. Zasadzinski, C. Rispe, D. Tagu, AphidBase: A database for aphid genomic resources. *Bioinformatics* **23** (2007).

60. J. Hallgren, *et al.*, DeepTMHMM predicts alpha and beta transmembrane proteins using deep neural networks. *bioRxiv* (2022).

61. I. Letunic, S. Khedkar, P. Bork, SMART: Recent updates, new developments and status in 2020. *Nucleic Acids Res* **49** (2021).

62. F. Teufel, *et al.*, SignalP 6.0 predicts all five types of signal peptides using protein language models. *Nat Biotechnol* **40** (2022).

63. M. H. Høie, *et al.*, NetSurfP-3.0: accurate and fast prediction of protein structural features by protein language models and deep learning. *Nucleic Acids Res* **50** (2022).

64. S. Lu, *et al.*, CDD/SPARCLE: The conserved domain database in 2020. *Nucleic Acids Res* **48** (2020).

65. K. Tamura, G. Stecher, S. Kumar, MEGA11: Molecular Evolutionary Genetics Analysis Version 11. *Mol Biol Evol* **38** (2021).

66. T. Horn, M. Boutros, E-RNAi: A web application for the multi-species design of RNAi reagents-2010 update. *Nucleic Acids Res* **38** (2010).

67. M. W. Pfaffl, A new mathematical model for relative quantification in real-time RT–PCR. *Nucleic Acids Res* **29** (2001).

Figure Legends

Figure 1. Diurnal rhythmicity of aphid feeding behaviors. The number of honeydew droplets produced by aphids was measured at the end of each 12 h day and night cycle for 48 h. Aphid assays were conducted on wheat plants (A) and artificial diet (B). Asterisks indicate significant differences between treatments (Mann-Whitney test, *p<0.05, ***p<0.001). Aphid feeding activity was monitored every 4h over a 24h period. The total time (minute) spent by the aphid in phloem salivation (E1) and phloem ingestion (E2) are represented in box plots (C, D). Solid lines, boundaries, and whiskers indicate the median, 25th, and 75th percentiles and 1.5 interquartile ranges, respectively. Points indicate outliers. Different letters above the boxes denote significant differences (Kruskal-Wallis test corrected by Bonferroni for multiple comparisons, adj. p<0.05). Diurnal rhythmicity of E1 (C) and E2 (D) waveforms over 24 hours was assessed with COSINOR, using a curved line for the fitted sinusoidal curve and a shaded area for the 95% confidence band. Significance is only established for a diurnal rhythm if the COSINOR p-value is <0.05. Yellow and black bars at the x-axis mirror the day and night. ZT = Zeitgeber time.

Figure 2. Diurnal rhythmicity of gene expression in *R. padi* and their roles in aphid feeding. (A) Rose diagram displaying acrophase frequency of diurnally rhythmic transcripts in *R. padi*. Each bar represents the number of rhythmic sequences with acrophase values in each 24 h period. Yellow and gray areas indicate day and night, respectively. Numbers around the outer sphere indicate zeitgeber time (ZT). (B) Soft-clustering of diurnally rhythmic transcripts in *R. padi*. Membership scores, color-coded with red, yellow, and blue, represent high, medium, and low membership values. Gray areas in each cluster represent the night. (C) Top-10 significantly enriched KEGG pathways for diurnally rhythmic transcripts in each cluster. Circle size and color represent genes enriched in a KEGG pathway, and Benjamini-Hochberg adjusted p-value, respectively. Gene ratio indicates the percentage of diurnally rhythmic transcripts of a cluster. (D-E) Daily expression profile of two diurnally rhythmic osmoregulatory genes, aquaporin 1 (AQP1) and gut sucrase 1 (SUC1). Solid lines, boundaries, and whiskers of each box indicate median, 25th, and 75th percentiles and 1.5 interquartile ranges. Curved line and shaded area represent the fitted periodic sinusoidal curve and 95% confidence band. Yellow and black bars on the x-axis mirror day and night. (F) Kaplan-Meier survival curve and (G) fecundity of aphids after silencing AQP1 and SUC1. Significant differences were tested using a log-rank test with Benjamini-Hochberg adjustment and a general linear model with Tukey's multiple comparisons test, respectively (*adj. p<0.05, ***adj. p<0.001, ****adj. p<0.0001). (H) Number of honeydew droplets produced after silencing AQP1 and SUC1 on wheat. Yellow and black bars represent the average number of droplets produced at the end of each 12:12h day and night for 4 days. The dsRNA GFP (dsGFP) was used as negative control. Asterisks indicate significant differences between treatments (Mann-Whitney test, **p<0.01, ****p<0.0001). NS indicates no significant difference.

Figure 3. Diurnally rhythmic putative salivary effectors in *R. padi*. Temporal expression data of identified putative salivary effectors were analyzed for periodicity using COSINOR. (A) Heatmap displays temporal expression patterns of 42 diurnally rhythmic putative salivary effectors. Each row and column represent the salivary effectors and zeitgeber time (ZT), respectively. Yellow and black bars at x-axis mirror day and night. (B) Sankey plot illustrates significantly enriched GO terms associated with diurnally rhythmic putative salivary effectors. Node color corresponds to clade number in the heatmap (A).

Figure 4. *R. padi* performance on wheat and artificial diet after silencing diurnally rhythmic salivary effectors. (A) Identification of key salivary effectors for functional analysis. Yellow and black dots represent diurnally rhythmic effectors with acrophases during the day and night, respectively. C002 and E8696 (ranked in top-five of the highest amplitudes) are core transcripts due to their high clustering membership scores (>0.8). (B) Expression levels of C002 and E8696 in *R. padi* heads and bodies (without heads and nymphs). Statistical difference in gene expression between treatments was tested using a two-tailed *t*-test (*$p<0.05$, **$p<0.01$). (C-D) Temporal expression patterns of C002 and E8696 in *R. padi* over a 24h period. Solid line, boundaries, and whiskers of each box indicate the median, 25th and 75th percentiles, and 1.5 interquartile ranges, respectively. Curved line and shaded area represent the fitted periodic sinusoidal curve and 95% confidence band, respectively. (E) Kaplan-Meier survival curves and (F) fecundities of aphids on wheat plants after silencing salivary effector genes. (G) Kaplan-Meier survival curves and (H) fecundities of aphids on artificial feeding diets after silencing salivary effector genes. The significant differences in aphid survivorship and fecundity were tested using a log-rank test with Benjamini-Hochberg adjustment for false discovery rate and a general linear model with Dunnett's multiple comparisons test, respectively (*adj. $p<0.05$, **adj. $p<0.01$, ***adj. $p<0.001$, ****adj. $p<0.0001$). The number of honeydew droplets produced by aphids after silencing C002 and E8696 on wheat plant (I) and artificial diet (J). Yellow and black bars represent the mean number of honeydew drops produced at the end of each 12:12 h day and night for 4 days. Asterisk indicates significant differences between treatments (Mann-Whitney test, *$p<0.05$, **$p<0.01$, ****$p<0.0001$). (K) Aphid feeding activity was monitored using EPG technique. Average time spent by the aphid in E1 (phloem salivation) and E2 (phloem ingestion) are displayed in the bar graph (Mann-Whitney test, *$p<0.05$, **$p<0.01$).

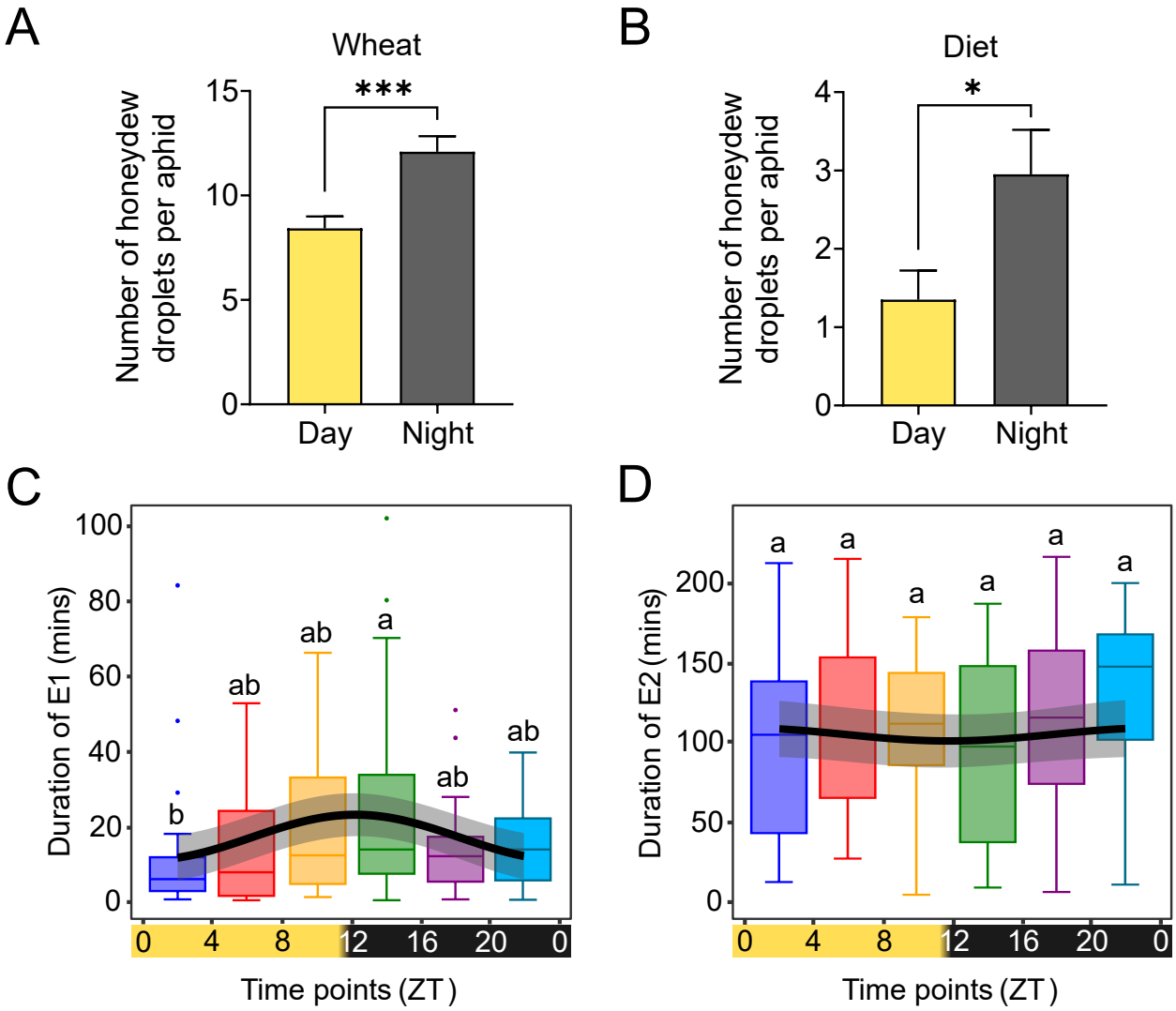
A
Wheat
***
Number of honeydew droplets per aphid
15
10
5
0
Day
Night
B
Diet
*
Number of honeydew droplets per aphid
4
3
2
1
0
Day
Night
C
Duration of E1 (mins)
100
80
60
40
20
0
b
ab
ab
a
ab
ab
0
4
8
12
16
20
0
Time points (ZT)
D
Duration of E2 (mins)
200
150
100
50
0
a
a
a
a
a
a
0
4
8
12
16
20
0
Time points (ZT)

Figure 1

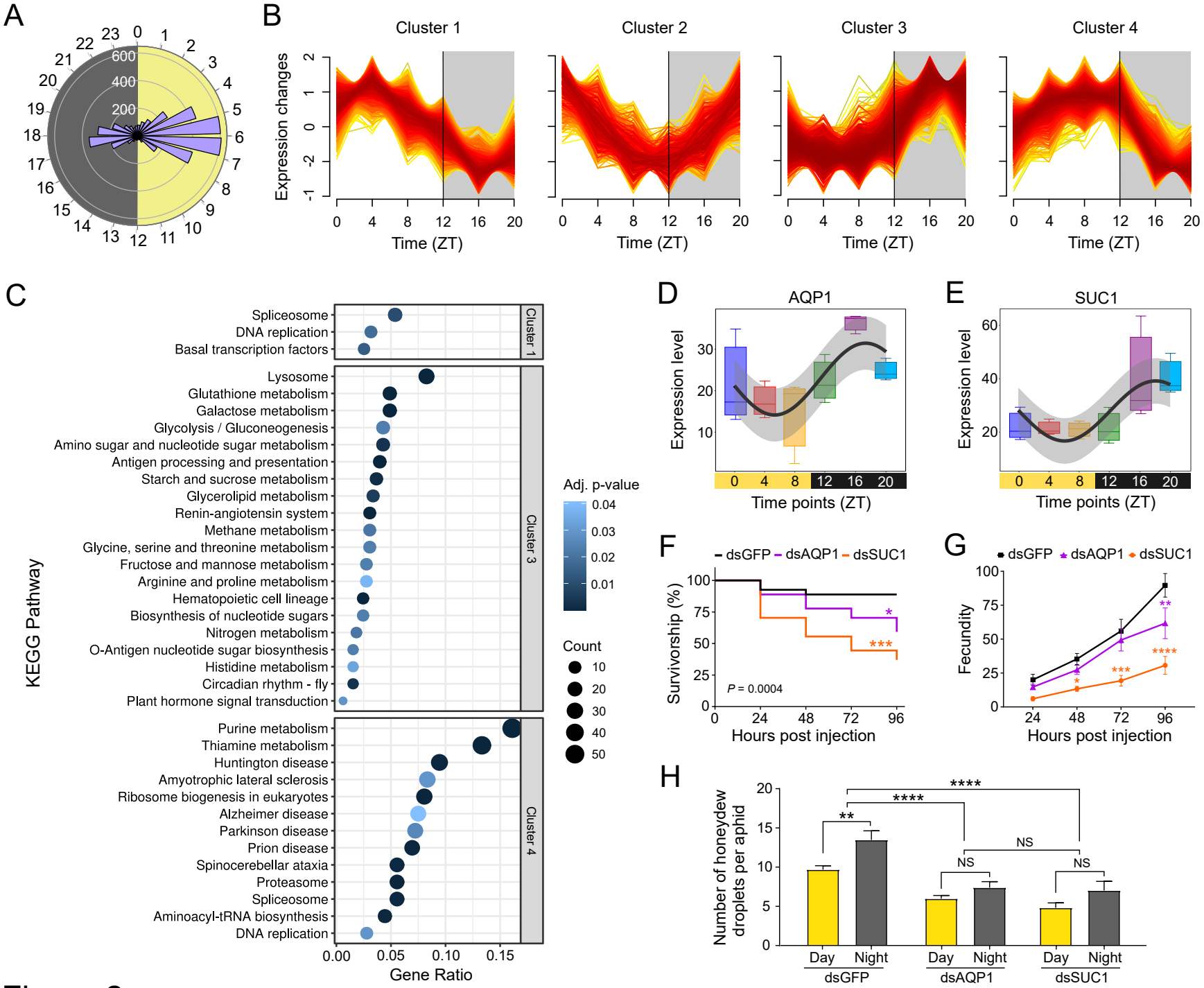
A
B
Cluster 1
Cluster 2
Cluster 3
Cluster 4
Expression changes
Time (ZT)
C
KEGG Pathway
Spliceosome
DNA replication
Basal transcription factors
Lysosome
Glutathione metabolism
Galactose metabolism
Glycolysis / Gluconeogenesis
Amino sugar and nucleotide sugar metabolism
Antigen processing and presentation
Starch and sucrose metabolism
Glycerolipid metabolism
Renin-angiotensin system
Methane metabolism
Glycine, serine and threonine metabolism
Fructose and mannose metabolism
Arginine and proline metabolism
Hematopoietic cell lineage
Biosynthesis of nucleotide sugars
Nitrogen metabolism
O-Antigen nucleotide sugar biosynthesis
Histidine metabolism
Circadian rhythm - fly
Plant hormone signal transduction
Purine metabolism
Thiamine metabolism
Huntington disease
Amyotrophic lateral sclerosis
Ribosome biogenesis in eukaryotes
Alzheimer disease
Parkinson disease
Prion disease
Spinocerebellar ataxia
Proteasome
Spliceosome
Aminoacyl-tRNA biosynthesis
DNA replication
Gene Ratio
Adj. p-value
Count
D
AQP1
Expression level
Time points (ZT)
E
SUC1
F
dsGFP
dsAQP1
dsSUC1
Survivorship (%)
P = 0.0004
Hours post injection
G
Fecundity
H
Number of honeydew droplets per aphid
Day
Night
NS

Figure 2

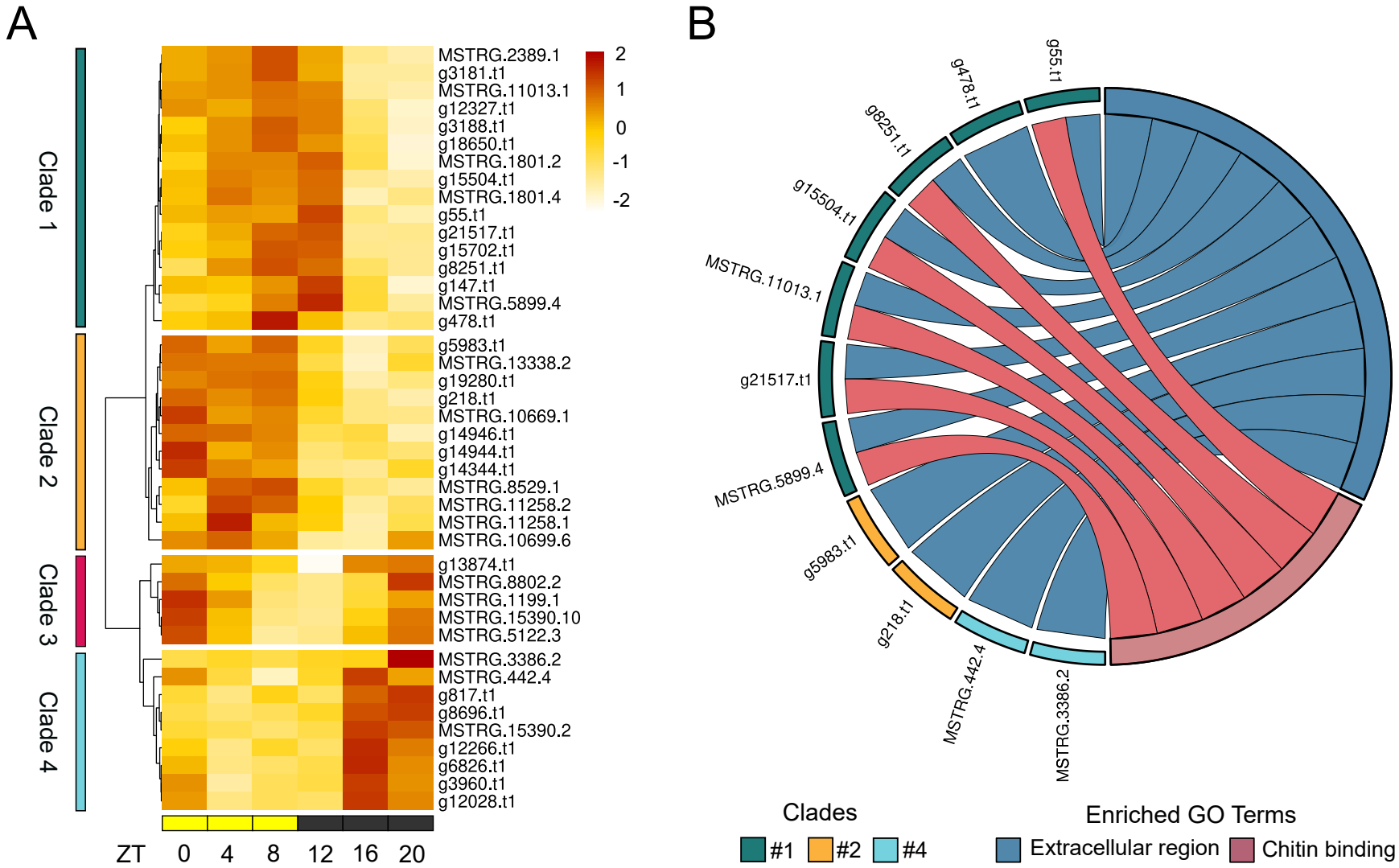
A
Clade 1
Clade 2
Clade 3
Clade 4
MSTRG.2389.1
g3181.t1
MSTRG.11013.1
g12327.t1
g3188.t1
g18650.t1
MSTRG.1801.2
g15504.t1
MSTRG.1801.4
g55.t1
g21517.t1
g15702.t1
g8251.t1
g147.t1
MSTRG.5899.4
g478.t1
g5983.t1
MSTRG.13338.2
g19280.t1
g218.t1
MSTRG.10669.1
g14946.t1
g14944.t1
g14344.t1
MSTRG.8529.1
MSTRG.11258.2
MSTRG.11258.1
MSTRG.10699.6
g13874.t1
MSTRG.8802.2
MSTRG.1199.1
MSTRG.15390.10
MSTRG.5122.3
MSTRG.3386.2
MSTRG.442.4
g817.t1
g8696.t1
MSTRG.15390.2
g12266.t1
g6826.t1
g3960.t1
g12028.t1
2
1
0
-1
-2
ZT 0 4 8 12 16 20
B
g55.t1
g478.t1
g8251.t1
g15504.t1
MSTRG.11013.1
g21517.t1
MSTRG.5899.4
g5983.t1
g218.t1
MSTRG.442.4
MSTRG.3386.2
Clades
#1
#2
#4
Enriched GO Terms
Extracellular region
Chitin binding

Figure 3

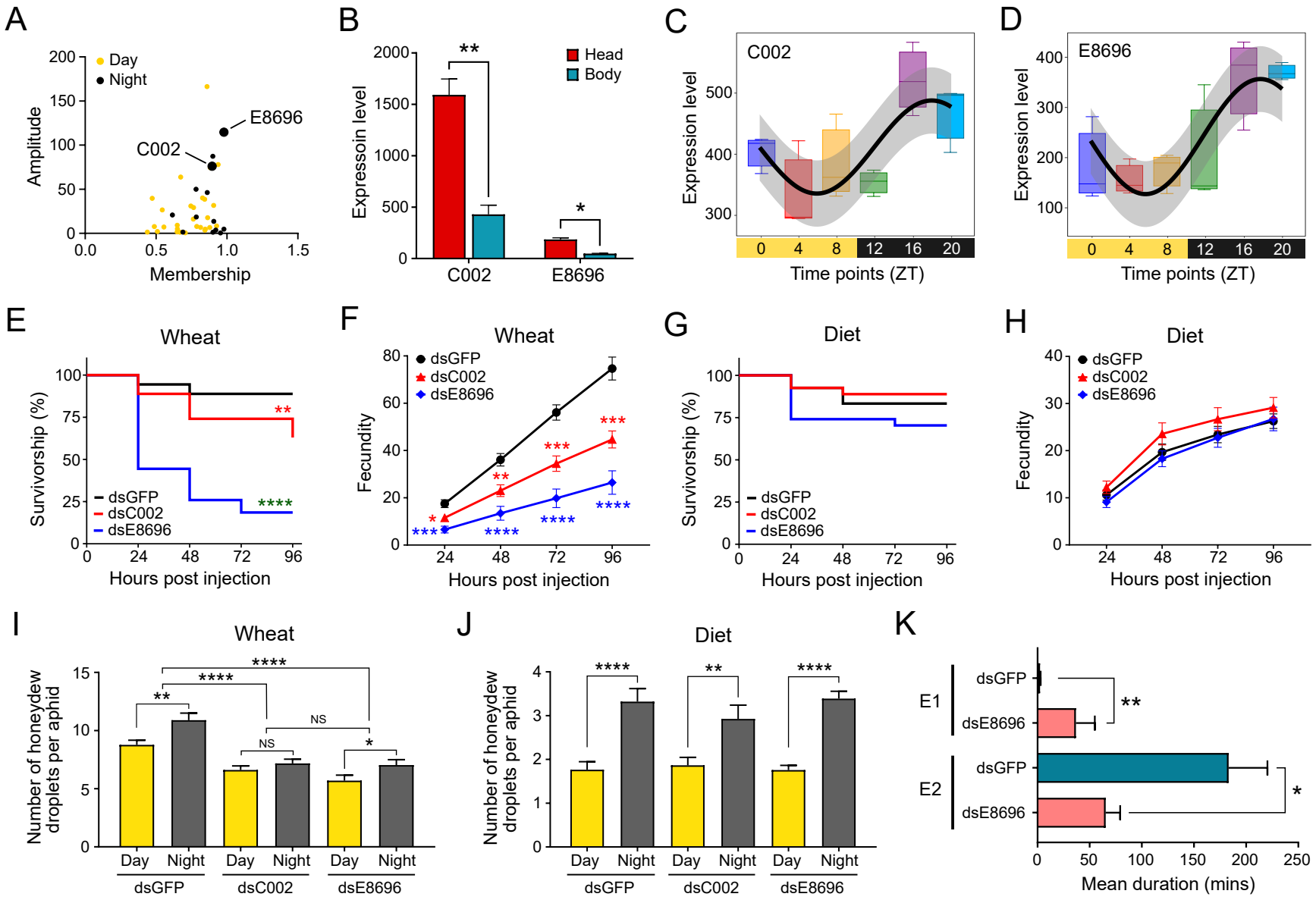
A
Day
Night
E8696
C002
Amplitude
Membership
B
Head
Body
Expressoin level
C002
E8696
C
C002
Expression level
Time points (ZT)
D
E8696
Expression level
Time points (ZT)
E
Wheat
Survivorship (%)
dsGFP
dsC002
dsE8696
Hours post injection
F
Wheat
Fecundity
dsGFP
dsC002
dsE8696
Hours post injection
G
Diet
Survivorship (%)
dsGFP
dsC002
dsE8696
Hours post injection
H
Diet
Fecundity
dsGFP
dsC002
dsE8696
Hours post injection
I
Wheat
Number of honeydew droplets per aphid
Day
Night
dsGFP
dsC002
dsE8696
NS
J
Diet
Number of honeydew droplets per aphid
Day
Night
dsGFP
dsC002
dsE8696
K
E1
E2
dsGFP
dsE8696
Mean duration (mins)

Figure 4